Suppression of error-field-induced magnetic islands by Alfvén resonance effect in rotating plasmas

2009 Nucl. Fusion 49 075018

(http://iopscience.iop.org/0029-5515/49/7/075018)

IOP Publishing and International Atomic Energy Agency Nuclear Fusion
Nucl. Fusion **49** (2009) 075018 (6pp) doi:10.1088/0029-5515/49/7/075018

Suppression of error-field-induced magnetic islands by Alfvén resonance effect in rotating plasmas

M. Furukawa[1] **and L.-J. Zheng**[2]

[1] Graduate School of Frontier Sciences, The University of Tokyo, Kashiwa, Chiba 277-8561, Japan
[2] Institute for Fusion Studies, University of Texas at Austin, Austin, TX 78712, USA

E-mail: furukawa@k.u-tokyo.ac.jp

Received 31 December 2008, accepted for publication 8 May 2009
Published 8 June 2009
Online at stacks.iop.org/NF/49/075018

Abstract
Error-field penetration is numerically studied in cylindrical tokamak geometry with plasma rotation. For a static error field, non-rotating magnetic islands are generated in the steady state. The penetrated perturbed magnetic flux is effectively reduced by the plasma rotation at small resistivity. Twin current sheets are formed at the Alfvén resonance positions when the plasma rotation is fast enough, and thereby the error-field penetration is significantly changed. The electromagnetic torque increases linearly in the plasma rotation velocity especially at high rotation velocity and low resistivity regime, which agrees with previous theoretical prediction, although the linear scaling can be easily affected if the Alfvén resonance is located close to the plasma edge. The electromagnetic torque in this regime does not depend on the resistivity. For high beta or small resistivity plasmas, the resultant volume-integrated electromagnetic torque, which brakes the plasma rotation, becomes maximum at very small, almost zero experimentally, rotation velocity.

PACS numbers: 52.35.Py, 52.55.Fa, 52.55.Tn

1. Introduction

Interaction between magnetic islands and the externally applied non-symmetric fields, such as error fields in tokamaks, has been paid much attention in tokamak plasma research. For example, locked modes [1] observed in tokamak experiments can degrade the confinement and can also precede disruptions. Such mode locking can occur even in low density discharges.

Such an error field can be amplified by the response of the plasma [2, 3]. If the error field is in resonance with a rational surface inside the plasma, one can expect that magnetic islands are generated at the rational surface. The response of the plasma to the error field has been studied, and it was shown that the plasma rotation shields the penetration of the error field into the plasma [4–9]. When the plasma rotation is included, the Alfvén frequency is Doppler shifted. Then the singularity occurs at positions where the Doppler shifted Alfvén frequency becomes zero ($m\Omega_p + n\Omega_t = \pm k_\parallel v_A$ where m and n are the poloidal and toroidal mode numbers, respectively, Ω_p and Ω_t are the poloidal and toroidal plasma rotation frequency, $k_\parallel$ denotes the wave number parallel to the ambient magnetic field and v_A is the Alfvén velocity), not at the rational surface where the original Alfvén frequency is zero ($k_\parallel v_A = 0$). The plasma resistivity can have a finite effect at the Alfvén resonances or the singularities of the governing equations without dissipation, and resistive layers are generated at the resonances. When the distance between the two Alfvén resonances is wide enough compared with the width of the resistive layers, the resistivity has little effect at the mode-resonant surface and the plasma inertia dominates the dynamics there. Therefore, the penetration of the externally given error field into the plasma is significantly affected in this parameter regime. In other words, the inner-layer response to the error field changes drastically when the plasma rotation is fast enough.

The magnetic perturbation penetrating inside the plasma exerts an electromagnetic torque which works to slow down the plasma rotation. By balancing the electromagnetic torque with a viscous torque, which originates from the discontinuity in the first radial derivative of the flow velocity across the magnetic islands, one can obtain a stationary state. If the torque balance is lost because of a gradual change in a plasma parameter such as the plasma rotation velocity, the plasma exhibits

the bifurcation phenomenon where the nonlinear magnetic islands suddenly open up and the plasma rotation velocity is significantly reduced. This bifurcation phenomenon is used in explaining the experimental results [10, 11].

The effect of the Alfvén resonances to the formation of magnetic islands and the generation of a torque was studied experimentally [12], numerically [5, 7, 13, 14] as well as theoretically [4, 6, 8, 9, 15]. In [12], penetration of rotating resonant error field into the plasma was studied by experiments as well as by simulations. The situation is equivalent to a system of rotating plasma with static error field. As stated in their paper, this might be in the so-called 'visco-resistive regime' since a clear signature of the Alfvén resonance was not observed. In [7], resistive magnetohydrodynamics (MHD) equations are solved numerically in a slab geometry with a perturbed boundary, and damping of the plasma rotation at the Alfvén resonances was observed. Two kinds of steady states have been found: large magnetic islands exist with strongly damped plasma rotation and no magnetic island with fast plasma rotation. The viscosity and resistivity were not small values. In [6, 8], it was theoretically shown that the penetration of magnetic perturbation is shielded by the plasma rotation. The resultant electromagnetic torque was shown to be proportional to the plasma rotation velocity [6, 8, 9]. In [15], it was shown that the Alfvén resonances generate a torque even in an ideal plasma. Recently the nonlinear evolution of driven magnetic islands in rotating plasmas was studied numerically [14], and a clear Alfvén resonance effect was found in the simulation results. In their simulation, the equilibrium plasma rotation as well as the magnetic field profile can change. Also the magnetic perturbation at the plasma edge is increased in time to drive the magnetic reconnection. The system evolves dynamically in their study and no stationary state is obtained since it is driven continuously and the equilibrium components change in time.

In this paper, we study the error-field penetration in rotating cylindrical plasmas numerically. The parameter regime extends from the so-called visco-resistive regime to the inertial regime, where the resistivity and viscosity are small enough so that the twin Alfvén resonances are well separated and the dissipation does not play an important role at the rational surface. It is noted that numerical results in slab geometry [16] were shown to agree well with the analytic expression [6, 9] in the so-called visco-resistive regime. We find numerically that the volume-integrated electromagnetic torque in the inertial regime scales linearly in the plasma rotation velocity at the mode-resonant surface, which agrees with the theoretical prediction, while on the other hand, that such a scaling can be easily changed if the resonant surface is located near the plasma edge. It is also found that the peak of the electromagnetic torque in the slow rotation regime, which is used in explaining the experimental results of resistive wall modes, moves towards zero rotation as the resistivity is decreased. For high beta or low resistivity plasma, the peak seems to appear at very slow, or almost zero experimentally, rotation by this simple model calculation.

In order to study such parameter dependence of the error-field penetration, the reduced MHD equation is solved as an initial value problem in the presence of a given magnetic perturbation at the plasma edge. The numerical code is used just for obtaining a stationary state, if it exists, for the edge perturbation; we will focus only on such stationary states and do not discuss the transient time evolution in this paper. It is also noted that the equilibrium magnetic field and plasma rotation are kept unchanged in time, instead of changing them, which leads to dynamic evolution of the system. Then we obtain the island width, the phase, the electromagnetic torque and so on as a function of plasma rotation velocity. If we can assume that the change in equilibrium quantities is slow enough, then those quantities can be regarded just as parameters; the system may slowly evolve in a quasi-stationary manner. Thus it is meaningful to focus only on the stationary states.

The paper is organized as follows. In section 2, the setting of the simulation is explained. The numerical results are shown in section 3. Conclusions are given in section 4.

2. Simulation settings

In this study, the low-beta reduced MHD equation is solved in cylindrical geometry. The conventional cylindrical coordinates $(r,\ \theta,\ z)$ are used. The length of the plasma column is $2\pi R_0$. The reduced MHD equation is normalized by using the plasma minor radius a, the magnetic field in the z direction B_0, the Alfvén velocity $v_\mathrm{A} := B_0/\sqrt{\mu_0\rho}$, where μ_0 is the vacuum permeability and ρ is the mass density, and the Alfvén time $\tau_\mathrm{A} := a/v_\mathrm{A}$. The inverse aspect ratio is defined as $\varepsilon := a/R_0$. The magnetic and velocity fields are expressed by $\boldsymbol{B} = \hat{\boldsymbol{z}} + \nabla_\perp\psi \times \hat{\boldsymbol{z}}$ and $\boldsymbol{v} = \hat{\boldsymbol{z}} \times \nabla_\perp\varphi$, respectively, where $\hat{\boldsymbol{z}}$ is the unit vector in the z direction. The reduced MHD equations are written as

$$\frac{\mathrm{d}U}{\mathrm{d}t} = -\nabla_\parallel J + \nu\nabla_\perp^2 U, \tag{1}$$

$$\frac{\partial\psi}{\partial t} + \nabla_\parallel\varphi = \eta\nabla_\perp^2\psi. \tag{2}$$

Here, $\nabla_\perp$ denotes the derivative in the r–z plane, $U := \nabla_\perp^2\varphi$ is the vorticity in the z direction, $J := \nabla_\perp^2\psi$ is the current in the $-z$ direction, ν and η are the viscosity and resistivity, respectively, the total time derivative is defined by $\mathrm{d}/\mathrm{d}t := \partial/\partial t + [\varphi,\ ]$ and the parallel derivative is defined by $\nabla_\parallel = \partial/\partial z - [\psi,\ ]$, where the Poisson bracket is defined by $[f, g] := \hat{\boldsymbol{z}} \cdot \nabla f \times \nabla g$. These equations are solved numerically by using the finite-difference method in the r direction, Fourier-series expansion in the θ and z directions as $\mathrm{e}^{\mathrm{i}(m\theta - n\varepsilon z)}$ and the Runge–Kutta method with step-size control for time integration. The mesh accumulation technique was used if necessary.

The equilibrium magnetic field is given by a toroidal current density $j_\mathrm{t}(r) = j_{\mathrm{t}0}(1 - r^2)^3$. The constant parameter $j_{\mathrm{t}0}$ was chosen so that the safety factor q at the plasma edge becomes $q_a = 3$. Then, the $q = 2$ surface is located at $r = 0.811$: this radius is denoted by r_s hereafter. The equilibrium plasma rotation is assumed to be in the poloidal direction in this study. In tokamak plasmas, poloidal rotation is considered to be damped neoclassically and the rotation is mainly in the toroidal direction. However, the important ingredient in this study is the split of the Alfvén resonances, which can be introduced either by toroidal rotation or by poloidal rotation as shown briefly in the introduction, i.e. $m\Omega_\mathrm{p} + n\Omega_\mathrm{t} = \pm k_\parallel v_\mathrm{A}$. Thus the poloidal rotation is used.

The poloidal plasma rotation velocity profile is assumed to be $v_\theta(r) = v_{\theta s} r/r_s$ where $v_{\theta s}$ is a constant. The inverse aspect ratio was set to $\varepsilon = 1/10$. Finally, $\nu = 10^{-7}$ was used and η was changed for several values.

The tearing mode parameter Δ', the logarithmic jump of the perturbation ψ, for $m/n = 2/1$ mode is -0.132 under the fixed boundary condition, and is 2.96 under the no-wall condition.

The equilibrium component of ψ is assumed to be zero at the magnetic axis $r = 0$. Then it has a finite value at the plasma edge $r = 1$. Especially for the present case, $\psi_{0/0}(1) = 0.0347$. The magnetic perturbation at the plasma edge is given so that $\psi_{2/1}(1)/\psi_{0/0}(1) = \frac{1}{2} \times 10^{-3}$. This value is kept unchanged in the simulation. For the radial profile of the initial perturbation, $\psi_{2/1}(r)$ is assumed to be proportional to r^2, which is the vacuum field for the $m = 2$ mode. For the stream function of the velocity field φ, the edge value was given by $\varphi_{2/1}(1) = c\psi_{2/1}(1)$, where the constant c was chosen so that it satisfies the linearized ideal Ohm's law with $\partial/\partial t = 0$. Then, the initial perturbation of $\varphi_{2/1}$ inside the plasma region was set to be $\varphi_{2/1}(r) = c\psi_{2/1}(r)$.

As explained in the introduction, the numerical code was used just for obtaining a stationary state, if it exists, for a given edge perturbation; we will focus only on such stationary states and not discuss the transient time evolution in this paper. As a reference, several examples of time evolution to reach the stationary states are shown in appendix A. In order to investigate the parameter dependence, the equilibrium magnetic field and plasma rotation are kept unchanged in time. If stationary states are reached, for example, at various plasma rotation velocities eventually, then we can summarize the dependence of the island width, phase, electromagnetic torque and so on as a function of plasma rotation velocity. If we can assume that the change in equilibrium quantities is slow enough, or if the system does not evolve so dynamically, then this parametrization is meaningful since the system may evolve slowly in a quasi-stationary manner.

3. Alfvén resonance effect on the error-field-induced islands and electromagnetic torque

Figure 1 shows the radial profile of $\psi_{2/1}$ at the stationary state for $\eta = 10^{-5}$. Plasma rotation velocities are chosen to be $v_{\theta s} = 10^{-4}$, 10^{-3} and 10^{-2}. For $v_{\theta s} = 10^{-4}$, the mode structure is similar to the ordinary tearing mode. The edge magnetic perturbation is amplified in the plasma. In contrast, for $v_{\theta s} = 10^{-3}$ and 10^{-2}, the penetration of the magnetic perturbation is suppressed significantly, and $\psi_{2/1}$, especially its real part, becomes almost zero at $r < r_s$. Since these profiles are obtained as stationary states, the magnetic islands are not rotating. This situation seems to be classified in a suppressed island interacting with a given static error field, where its slip frequency can be large [6]. The values of rotation velocity used here are categorized in the visco-resistive, resistive-inertial and inertial regimes for $v_{\theta s} = 10^{-4}$, 10^{-3} and 10^{-2}, respectively.

Figure 2 shows the radial profile of $\psi_{2/1}$ and $J_{2/1}$ at the stationary state for $\eta = 10^{-7}$. Plasma rotation velocities are chosen to be $v_{\theta s} = 10^{-4}$, 10^{-3} and 10^{-2} again. In this case, the edge magnetic perturbation, especially the real part of $\psi_{2/1}$, is

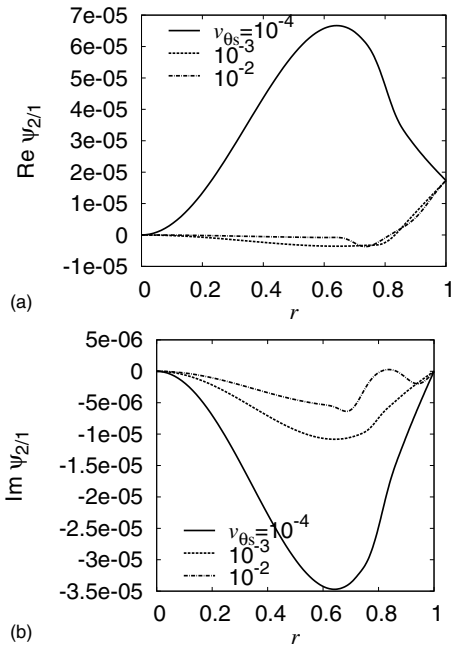

Figure 1. $\psi_{2/1}$ for $\eta = 10^{-5}$. (*a*) Re $\psi_{2/1}$ and (*b*) Im $\psi_{2/1}$.

shielded out strongly, and $\psi_{2/1}$ becomes almost zero at $r < r_s$ for $v_{\theta s} = 10^{-4}$. For $v_{\theta s} = 10^{-2}$, on the other hand, the real part of $\psi_{2/1}$ has a finite value between the Alfvén resonance at the smaller r side and the rational surface. These stationary states are also considered as the suppressed island states. The values of rotation velocity are categorized in the visco-resistive regime for $v_{\theta s} = 10^{-4}$ and 10^{-3}, and the inertial regime for $v_{\theta s} = 10^{-2}$.

This shielding is related to the generation of localized current at the rational surface and/or the Alfvén resonances. It is easy to recognize especially for $v_{\theta s} = 10^{-2}$ that two peaks exist in $J_{2/1}$, whose location is at the Alfvén resonances. They are related to the sharp spatial change in $\psi_{2/1}$. It is noted that, although $\psi_{2/1}$ becomes almost zero at the rational surface, especially the imaginary part of $\psi_{2/1}$ has a finite value in almost the entire plasma region.

The penetrated perturbed magnetic flux $|\psi_{2/1}(r_s)|$ and the phase of the O-point, if the formula of the constant-ψ magnetic island $w := 4(rq|\tilde{B}_r|/mq'B_\theta)_s^{1/2}$ [19] is used, is plotted in figure 3. These islands are not rotating with the equilibrium plasma rotation. Therefore, this situation seems to be the suppressed island state which was treated by linear layer response [6]. It is noted that the horizontal axis is in the log scale. We see that suppression of the penetrated magnetic flux by the plasma rotation is effective for smaller η; $|\psi_{2/1}(r_s)|$ is reduced significantly even at small plasma rotation velocity $v_{\theta s}$.

At large $v_{\theta s}$, the separation of the twin Alfvén resonances is much wider than the resistive layer. Thus we observe such twin current sheets in a distinguishable manner. At very small $v_{\theta s}$, we could not obtain a stationary state for $\eta = 10^{-7}$.

The phase of the O-point is located at $\pi/4$ at small $v_{\theta s}$. As the rotation velocity $v_{\theta s}$ is increased, the island phase is dragged in the direction of the plasma rotation. It is noted again that these islands are not rotating. For smaller η, the

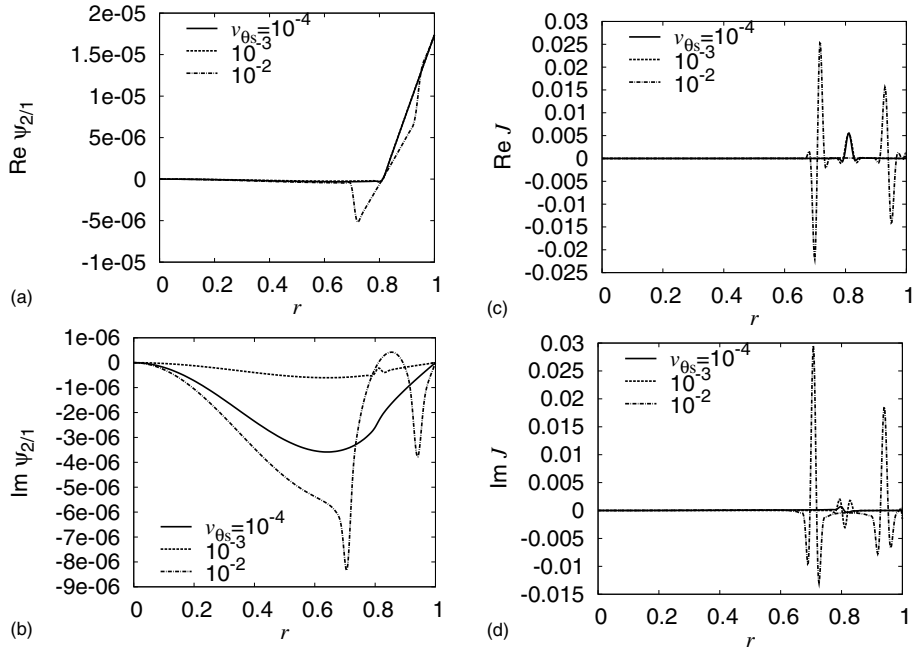

Figure 2. $\psi_{2/1}$ and $J_{2/1}$ for $\eta = 10^{-7}$. (*a*) Re $\psi_{2/1}$, (*b*) Im $\psi_{2/1}$, (*c*) Re $J_{2/1}$ and (*d*) Im $J_{2/1}$.

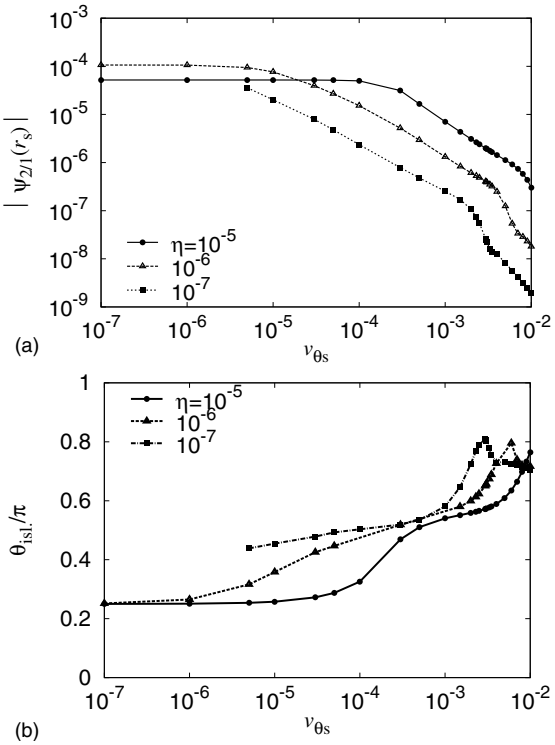

Figure 3. The penetrated perturbed magnetic flux $|\psi_{2/1}(r_s)|$ and the phase of the O-point if the formula of constant-ψ magnetic island $w := 4(rq|\tilde{B}_r|/mq'B_\theta)_s^{1/2}$ is used at stationary states. The horizontal axis is in log scale. (*a*) Penetrated perturbed magnetic flux $|\psi_{2/1}(r_s)|$. (*b*) Phase of the O-point.

island phase can be easily changed by smaller plasma rotation, which is accompanied by the reduction in the island width. The reason for the non-monotonic behaviour at large $v_{\theta s}$ is not identified yet.

The mechanism of the island saturation seems to be the quasi-linear effect, since the equilibrium magnetic and velocity fields are kept unchanged in the simulation. Then a question might be why the island width or the penetrated perturbed magnetic flux at the quasi-linear saturation depends on the resistivity at very low equilibrium rotation frequency. A kind of numerical proof cannot be presented unfortunately, as explained below, however, the key point may be that the magnetic perturbation is finite at the plasma edge. Let us first consider a situation where the perturbation is set to be zero at the plasma boundary. Then we can compute the so-called tearing mode parameter Δ' as a function of the distance from the mode-resonant surface x. If $\lim_{x\to 0}\Delta' > 0$ and $\Delta'(x = w) = 0$, then the perturbation will grow initially and the magnetic island width will saturate at $x = w$. However, $\lim_{x\to 0}\Delta' < 0$ in our study. Therefore, we cannot perform such conventional simulation of quasi-linear saturation. Next let us consider the situation with finite perturbation at the plasma edge. Since the teaing mode parameter Δ' under the free boundary condition is positive in our study, a perturbation can grow in the plasma in principle if we give a finite perturbation at the plasma edge. If a stationary state is reached, it is considered as a state where the free boundary behaviour and the response to a static error field (which is related to the ideal wall or fixed boundary behaviour) are mixed. Since the plasma resistivity changes the response to the static error field at the mode-resonant surface even at very low plasma rotation, it changes the ratio of the mixture of those two. This may explain the origin of the resistivity dependence of the island width at the low rotation regime. It is noted that the island width shows smooth dependence on resistivity as shown in appendix B.

It is noted that the plasma rotation profile is $v_\theta(r) = r\Omega_\theta$ with $\Omega_\theta =$ constant or a rigid rotation, and is kept unchanged in time. The width of the region where the ideal Ohm's law is

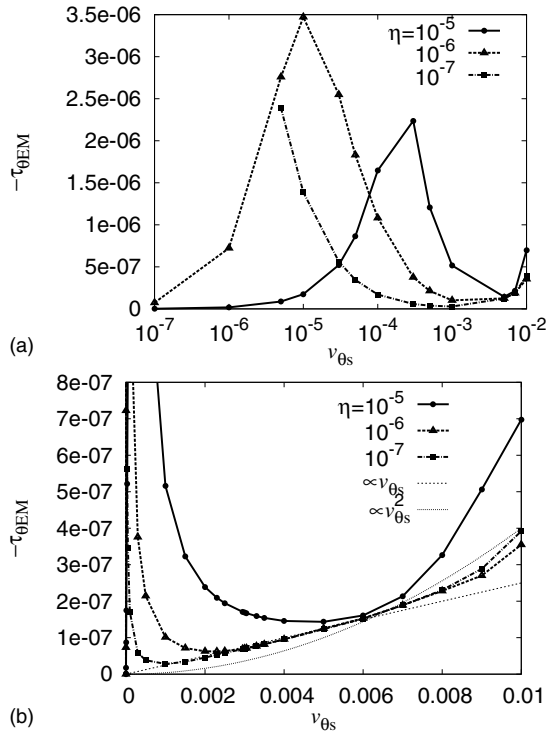

Figure 4. Volume-integrated electromagnetic torque. (*a*) Electromagnetic torque. The horizontal axis is in log scale. (*b*) Electromagnetic torque at the fast plasma rotation regime. The horizontal axis is in linear scale.

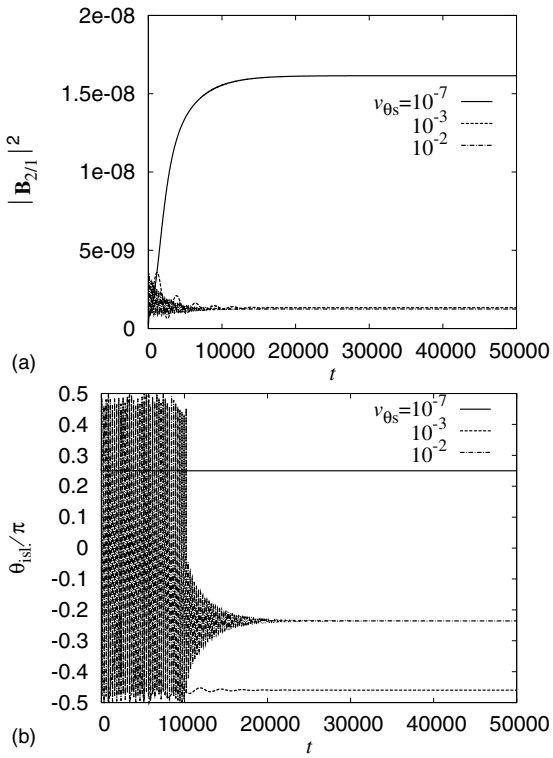

Figure A1. Time evolution of the perturbed magnetic energy and the phase for $\eta = 10^{-5}$. (*a*) $|\boldsymbol{B}_{2/1}|^2$. (*b*) Phase of the O-point of the magnetic island if the formula of constant-ψ magnetic island $w := 4(rq|\tilde{B}_r|/mq'B_\theta)_s^{1/2}$ is used.

not valid depends on the plasma resistivity. Therefore, when the resistivity is relatively large, the above rotation profile is maintained even in the island region with closed magnetic flux surface. It is noted that the larger island width observed for smaller resistivity at the low plasma rotation regime, even for the thinner resistive layer, seems to be due to the change in the mixture ratio of the free-boundary behaviour to the fixed-boundary behaviour as explained above.

Figure 4 shows the volume-integrated electromagnetic torque $\tau_{\theta EM}$. Since it brakes the plasma rotation and has negative values, $-\tau_{\theta EM}$ is plotted. It is noted that the horizontal axis is the log scale for figure 4(*a*) and is the linear scale for figure 4(*b*). The electromagnetic torque increases once and then decreases as $v_{\theta s}$ is increased at relatively small $v_{\theta s}$ regime. This electromagnetic torque profile is used in explaining the current experimental results of resistive wall modes by the forbidden band picture [11]. The peak of the electromagnetic torque moves towards smaller rotation velocity as the resistivity is decreased. For example, the torque becomes maximum around $v_{\theta s} = 10^{-5}$ for $\eta = 10^{-6}$, which might be almost zero experimentally.

As $v_{\theta s}$ is increased further, the torque starts to increase again. It is noted that $v_{\theta s} = 5 \times 10^{-3}$ is already in the inertial regime for $\eta = 10^{-6}$ and 10^{-7}. For $\eta = 10^{-5}$, $v_{\theta s} = 7 \times 10^{-3}$ is in the inertial regime, while $v_{\theta s} = 5 \times 10^{-3}$ is in the resistive-inertial regime but is close to the boundary between the resistive-inertial and the inertial regimes. If we look at this regime in the linear scale, figure 4(*b*), the torque seems to increase linearly in $v_{\theta s}$ especially around $10^{-3} \lesssim v_{\theta s} \lesssim 7 \times 10^{-3}$ for $\eta = 10^{-7}$. Two reference curves are plotted together; one is proportional to $v_{\theta s}$ and the other to $v_{\theta s}^2$. When $v_{\theta s}$ becomes so large, however, the torque deviates from the linear scaling even if $v_{\theta s}$ is in the inertial regime. It may be because the current sheet generated at one of the Alfvén resonances, at the larger r side, is sufficiently close to be affected by the plasma edge. As the resistivity becomes larger, the parameter regime where the linear scaling is observed becomes narrower since the inertial regime is obtained for faster plasma rotation.

4. Conclusions

We have investigated numerically the stationary state of the rotating plasma for a static edge magnetic perturbation in a cylindrical geometry. Non-rotating islands are obtained as stationary states for various plasma parameters. The penetration of the edge perturbation is strongly suppressed by the plasma rotation. At the fast plasma rotation velocity regime, the current sheets are generated at the Alfvén resonances which are well separated and the resistivity becomes ineffective at the rational surface. The resultant island width or the penetrated perturbed magnetic flux is significantly reduced, and the reduction by the rotation is more effective for smaller resistivity. The electromagnetic torque increases linearly in the rotation velocity for the fast rotation regime, which agrees with the previous theoretical prediction. However, this linear scaling seems to be easily changed if the resonant surface is located near the plasma edge. At the slow rotation velocity regime or the so-called visco-resistive regime, the electromagnetic torque has a maximum.

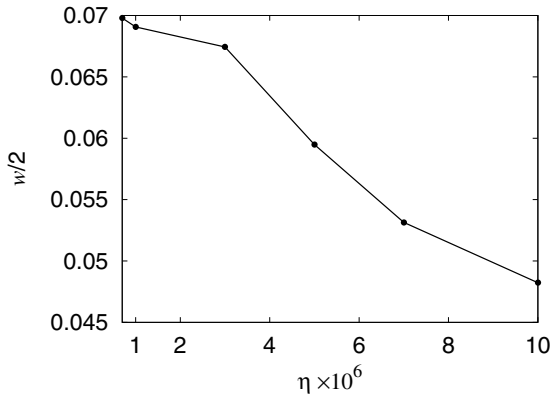

Figure B1. Island width against resistivity for $v_{\theta s} = 10^{-7}$.

The plasma rotation at the maximum moves towards zero rotation as the resistivity is decreased. In high beta or small resistivity plasmas, the maximum of the volume-integrated electromagnetic torque occurs at very small, almost zero experimentally, rotation velocity.

Acknowledgments

This work was supported by the Joint Institute for Fusion Theory (JIFT) exchange program and the Grant-in-Aid for Young Scientists (B) 19760595 (2007) from the Japan Society for the Promotion of Science (JSPS).

Appendix A. Stationary states

In this appendix, several numerical examples are shown of how the system reached the stationary states. Figure A1 shows the time evolution of the perturbed magnetic energy $|\boldsymbol{B}_{2/1}|^2$ and the phase of the O-point if the formula of the constant-ψ magnetic island $w := 4(rq|\tilde{B}_r|/mq'B_\theta)_s^{1/2}$ is used. The resistivity was $\eta = 10^{-5}$. It is seen that the simulation was run for a sufficiently long time that the system actually reaches the stationary state. The time required to obtain such a stationary state becomes longer as the resistivity is decreased. In figure A1(a), $|\boldsymbol{B}_{2/1}|^2$ grows and saturates without oscillation for $v_{\theta s} = 10^{-7}$; on the other hand, it evolves with oscillation for $v_{\theta s} = 10^{-3}$ and 10^{-2} and reaches a stationary value. The oscillation frequency is higher for faster $v_{\theta s}$. In figure A1(b), it is observed that the phase of the perturbation does not change in time; the island is not rotating. It is noted that $\theta_{\mathrm{isl.}}/\pi$ plotted in figure 3(b) is mapped in the range of $0 \leqslant \theta_{\mathrm{isl.}}/\pi < 1$ by adding a constant 0.5 if necessary.

Appendix B. Island width at slow rotation

This appendix is just for showing the dependence of the magnetic island width on the resistivity at slow plasma rotation. Figure B1 shows the island width in the stationary state against the resistivity at $v_{\theta s} = 10^{-7}$. Smooth dependence is observed.

References

[1] Scoville J.T. *et al* 1991 *Nucl. Fusion* **31** 875
[2] Boozer A.H. 2001 *Phys. Rev. Lett.* **86** 5059
[3] Boozer A.H. 2003 *Phys. Plasmas* **10** 1458
[4] Fitzpatrick R. and Hender T.C. 1991 *Phys. Fluids* B **3** 644
[5] Jensen T.H. *et al* 1991 *Phys. Fluids* B **3** 1650
[6] Fitzpatrick R. 1993 *Nucl. Fusion* **33** 1049
[7] Hurricane O.A., Jensen T.H. and Hassam A.B. 1995 *Phys. Plasmas* **2** 1976
[8] Boozer A.H. 1996 *Phys. Plasmas* **3** 4620
[9] Fitzpatrick R. 1998 *Phys. Plasmas* **5** 3325
[10] Gates D.A. and Hender T.C. 1996 *Nucl. Fusion* **36** 273
[11] Strait E.J. *et al* 2007 *Phys. Plasmas* **14** 056101
[12] Kikuchi Y., Uesugi Y., Takamura S. and Elfimov A.G. 2004 *Nucl. Fusion* **44** S28
[13] Wang X. *et al* 1998 *Phys. Plasmas* **5** 2291
[14] Ishii Y., Azumi M. and Smolyakov A.I. 2007 *Nucl. Fusion* **47** 1024
[15] Taylor J.B. 2003 *Phys. Rev. Lett.* **91** 115002
[16] Fitzpatrick R. 2003 *Phys. Plasmas* **10** 1782
[17] Strauss H.R. 1976 *Phys Fluids* **19** 134
[18] Hazeltine R.D. and Meiss J.D. 2003 *Plasma Confinement* (New York: Dover)
[19] Wesson J. 1997 *Tokamaks* (Oxford: Clarendon Press)